Local structure of NaNbO_{3}: A neutron scattering study

Lu Jiang, D. C. Mitchell, W. Dmowski, and T. Egami

Phys. Rev. B **88**, 014105 — Published 12 July 2013

DOI: 10.1103/PhysRevB.88.014105

Local structure of $NaNbO_3$: A neutron scattering study

Lu Jiang[1], D. C. Mitchell[1], W. Dmowski[2] and T. Egami[1,2,3]

[1] *Joint Institute for Neutron Sciences and Department of Physics and Astronomy, University of Tennessee, Knoxville, TN 37996, USA*
[2] *Joint Institute for Neutron Sciences and Department of Materials Science and Engineering, University of Tennessee, Knoxville, TN 37996, USA*
[3] *Oak Ridge National Laboratory, Oak Ridge, TN 37831, USA*

Abstract

We report the results of a neutron diffraction study of structural evolution in sodium niobate, $NaNbO_3$, which is the parent compound for lead-free ferroelectric material, as a function of temperature from 15 to 930 K over six phases. The Rietveld analysis of the high resolution powder neutron diffraction data shows the variation in the structure from cubic to rhombohedral ferroelectric structures. However, the refinements on local structure by the PDF method indicates that there are only three basic patterns of the local structure, and the ground states of $NaNbO_3$ in the low-temperature antiferroelectric and ferroelectric phases have the *R3c* symmetry, even though in the long range the system shows the *Pbcm* symmetry or the coexistence of two phases. The origin of the complex phase behavior and its implications on the performance as lead-free ferroelectrics are discussed.

Introduction

Ferroelectric materials are widely used in many electromechanical components and electronic devices, such as actuators, sensors, field-effect transistors and ultrasonic transducers. Due to strong piezoelectric response, $Pb(Zr,Ti)O_3$ (PZT) is the most widely employed ferroelectric materials at present, even though lead has recently been banned from many commercial applications and materials, for example, from solder, glass and pottery glaze, due to concerns regarding its toxicity. Therefore a concerted effort was mounted to develop lead-free piezoelectric ceramics. A large number of studies have been focused on the discovery of better ferroelectrics near the morphotropic phase boundaries (MPB) in alkaline niobate-based perovskite solid solutions[1-3]. In particular Saito, *et al*[4] have designed a new lead-free ferroelectrics based on the MPB in the perovskite-rich region of $(K,Na)NbO_3$, which shows excellent piezoelectric performance comparable to those of PZT. Interestingly their mother compound, sodium niobate, $NaNbO_3$, is known for its complex phase behavior, and there are a number of conflicting reports on its structure[5-22]. Thus there is a strong need for understanding the structure and phase transformation of sodium niobate.

At high temperatures $NaNbO_3$ takes the structure of simple perovskite. But as temperature is lowered[5-7], pressure is applied[8] or the sample size is reduced[9] $NaNbO_3$ undergoes a surprisingly complex sequence of structural phase transitions. Its rich phase diagram is generally described by Glazer and Megaw[10], which contains at least six phases, varying from cubic at high temperature, through tetragonal, orthorhombic and finally to rhombohedral structure below room temperature. This complexity invited many scientists to

study the temperature-induced phase changes in $NaNbO_3$ and its soft mode mechanism for structural change[11-17]. However, the results are seriously contradictory to each other, particularly at low temperatures. Above 913K, it has a paraelectric cubic phase *Pm3m*, and when cooling down, it evolves through a series of antiferrodistortive phases, tetragonal (T_2) *P4/mbm,*orthorhombic (T_1) *Cmcm,* orthorhombic (*S*) *Pbnm,* orthorhombic (*R*) *Pbnm,* orthorhombic (*P*) *Pbcm* phases, and forms a rhombohedral *R3c* phase at low temperatures. Mishra *et al*. replace the space group *Pnmm* of *S* and *R* phases with the *Pbnm* group according to a high-resolution powder neutron diffraction study.[18] They also point out that the antiferroelectric phase *Pbcm* and the ferroelectric phase *R3c* coexist and have competing interaction at room temperature and below[19]. Further in the transition mechanism, the high and room temperature phase transitions are considered to be due to the NbO_6 octahedral tilting, while the low temperature transitions are related to the off-centered displacements of niobium atoms and octahedral distortions of NbO_6[20-22]. In spite of extensive use of experimental techniques and theoretical studies, surprisingly large amounts of controversies are still present on details of the structure and process of phase transitions of $NaNbO_3$. In this article, we use the Rietveld and pair distribution function (PDF) analyses of high resolution neutron scattering data to probe the local structure of each phase and details of each phase of $NaNbO_3$.

Result and Discussion

1. Rietveld analysis of powder neutron diffraction data

Powder sample of $NaNbO_3$ (99.997% purity) was purchased from Alpha Aesar Co., and the pulsed neutron diffraction measurements were performed with the NPDF spectrometer of the Lujan Center of Los Alamos National Laboratory at various temperatures. The results were first analyzed using the Rietveld refinement (EXRGUI, revision 1225). The neutron diffraction pattern at 930K shown in Figure 1 was analyzed on the basis of an ideal cubic structure with the space group *Pm*3*m*. The cubic phase is well-fitted with the structural parameters of the ideal perovskite, with Na at (0,0,0), Nb at (0.5,0.5,0.5), O at (0.5,0.5,0) and $a = b = c = 3.9507$ Å. All the Bragg reflections present could be indexed as main cubic perovskite reflections. When temperature is lowered to 880K, the appearance of the superlattice peaks shown in Figure 1 indicates the phase transition to the tetragonal *P4/mbm* space group, which is induced by M and R zone boundary condensation involving the rotation of NbO_6 octahedra. Between 820K and 770K, $NaNbO_3$ has an orthorhombic *Cmcm* space group phase. The appearance of additional superlattice peaks (Figure 1) is the sign for phase transition and multiplicity of the unit cell. When temperature further goes down, numerous controversies are drawn on the space groups and phase transitions. As temperature falls in the range of 700K-600K, Ahtee *et al*.[6] find that it belongs to the *Pnmm* space group symmetry with the cell dimensions 2*2*2 with respect to the elementary perovskite cell by x-ray diffraction measurements. However, Mishra *et al*. argue that it undergoes a phase transition to the *Pbnm* space group with the $\sqrt{2}*\sqrt{2}*12$ cell dimensions at 700K and $\sqrt{2}*\sqrt{2}*6$ cell dimensions at 600K through neutron diffraction measurements. Our neutron diffraction patterns can be fitted well by the *Pbnm* space group parameters with $\sqrt{2}*\sqrt{2}*6$ cell

dimensions, partly supporting Mishra *et al*., but not much difference is seen between the patterns for 700K and 600K. Note that our model includes a small portion (4.5%) of a phase with *Cmcm* space group at 700K.

Between room temperature and 490K, the orthorhombic *Pbcm* space group seems to achieve the best fit in the Rietveld refinement. Below room temperature, as detected by Mishra *et al*., the orthorhombic *Pbcm* group and rhombohedra *R3c* group coexists within the entire temperature range, including the lowest temperature. If comparing every peak at low and room temperatures, it seems that most of the supperlattice peaks at low temperatures can find their original formation at room temperature, in spite of some shifts in the *Q* value and changes in intensity; still, some peaks are an exclusive result of the *R3c* space group symmetry, as shown in Figure 2. The evolution of phase transitions in our Rietveld refinement is shown in Table 1 and the lattice parameters, parameters of every atom position, thermal factor, phase fraction and the agreement factors are shown in Table 2.

Table 1. Phase evolution of $NaNbO_3$ at different temperatures by the Rietveld analysis

Temperature	930K	880K	820K-770K	700K	600K	490K-300K	190K-15K
Space group	*Pm3m*	*P4/mbm*	*Cmcm*	*Cmcm +Pbnm*	*Pbnm*	*Pbcm*	*Pbcm+R3c*
Symmetry	Cubic	Tetragonal	Orthorhombic			Orthorhombic (AFE)	Rhombohedra (FE)

2. Pair distribution function analysis above room temperature

In the antiferroelectric and ferroelectric phases $NaNbO_3$ undergoes lattice distortion, with tilting and atomic off-center displacements in the short range. However, the diffraction patterns are not sensitive to detailed local displacements during the phase transition. In order to determine differences between the local and average structures, the PDF method was employed to probe the evolution of the local structure, especially for those at temperatures below 490 K.

The PDF, denoted $g(r)$ in the following formula, describes all the interatomic distances present in the structure, and is obtained from the total structure function $S(Q)$ through the Fourier-transformation[23]:

$$g(r)-1=\frac{1}{2\pi^2 r\rho_0}\int_0^{+\infty} Q[S(Q)-1]\sin(Qr)dQ$$

Because $S(Q)$ includes both the Bragg and diffuse scattering intensities the PDF can describe aperiodic as well as periodic structure. From 900K to 600K, the PDF calculated (PDFGUI 1.0b) with the fitting parameters same as those in the Rietveld analysis shows good agreement with the experimental PDF, indicating that the crystallographic structure provides also a good description of the local atom arrangement above 600K. Figure 4 is an example of the experimental PDF agreeing with the calculated PDF using the Rietveld model at 820K. In Figure 3, within the basic cubic perovskite cell (around 4 Å), the two primary peaks correspond to Nb-O and Na-O are at r = 1.9 Å and r = 2.8 Å, which indicates that Nb is at the center of an NbO_6 octahedron and there is no obvious distortion in the unit cell.

When temperature is lowered to 490K, through the PDF analysis we find that the structure model obtained by the Rietveld refinement actually shows very poor agreement at small *r*, as shown in Figure 4, which suggests that for $r < 5.2$ Å the structure is actually not in the *Pbcm* space group. The PDF provides the data for true atomic distances which cannot easily be determined from the average structure analysis by the Rietveld analysis. If we use the parameters for the low temperature phase *R3c* group to refine all the atom positions and thermal factors, we can get excellent fit to the PDF below 5.2 Å as shown in Figure 5. The same conclusion is obtained through the PDF fitting from 490K to 300K. Therefore, in this range of temperature, the *Pbcm* space group describes only the long-range symmetries and atomic positions. On the other hand within the short range up to 5.2 Å, the correct local structure is surprisingly the *R3c* space group. This size of the domain is slightly smaller than the rhombohedral *R3c* unit cell, in which it keeps the character and symmetry of the *R3c* group, though distorted. These small *R3c* domains gradually stack into the *Pbcm* space group through the entire structure. Depending on the models resulted from the Rietveld refinement (detailed information given in Table 2), the *a* and *b* axises of the *Pbcm* unit cell rotate by 45° from those of the *R3c* unit cell; so it is most likely that the atoms form twin structures (as the Na and O atoms shown in figure 6) in *R3c* domains and along its diagonal direction, the whole structure can result in *Pbcm* symmetry. Moreover, the *R3c* space group is a ferroelectric phase while the *Pbcm* space group is antiferroelectric, which means that the local domains in the *R3c* group has a spontaneous polarization and they align in antiparallel arrangements to revolve into the *Pbcm* group. Along the *c* axis, the length of the *Pbcm* unit

cell (c = 15.48 Å) is about twice as the *R3c* unit cell (c = 7.82 Å) and about four times as the elementary cubic cell (3.95 Å), so every basic polarized cell also form similar twin structures to make the polarizations stack antiparallel through the whole structure as shown in Figure 6.

It is tradionally considered that the spontaneous polarization in ferroelectric and antiferroelectric phases of $NaNbO_3$ originates from the distortion of the lattice and off-centered displacement of Nb atoms. Figure 7 shows the PDF of $NaNbO_3$ at a very short range which is within the range of an elemental perovskite unit cell from 930K to 15K. We can see that the first peak, which corresponds to the Nb-O bond, is broad and asymmetric but without a split down to 600K (six green curves shown in Figure 7). As temperature falling down to 300K (four blue curves shown in Figure 7), the peak due to Nb-O bond is separated into two subpeaks, one around r = 1.9 Å and the other around r = 2.1 Å, and a Na-O bond peak appears at r = 2.4 Å as well. When the temperature is above 600K, where the structure is paraelectric, the Nb-O bond length is 1.95 Å, and the Na-O bond length is 2.8 Å. Therefore, in the antiferroelectric phases, the Nb atom in the octahedral NbO_6 is off-centered by 0.15 Å or 7.7%, while the Na atom in NaO_8 is off-centered by 0.4 Å or by 14%. This means Na has even a larger off-centered displacement than Nb, as shown in Figure 8, and both displacements contribute to the formation of local dielectric polarization.

3. Pair distribution function analysis at low temperatures

When $NaNbO_3$ is cooled down below room temperature, it exhibits ferroelectric behaviors due to the spontaneous polarization formed in its structure. A great deal of research has been focused on the structure in this range of temperature, and it is generally agreed that two phases, *R3c* and *Pbcm*, coexist. Our Rietveld analysis also shows the coexistence of the two phases. Two-phase coexistence in a compound at low temperatures usually signifies that at least one of the phases is metastable. The PDF analysis explained why this occurred.

As shown in Figure 9, if we use the model obtained from the Rietveld refinement, the PDF fitting confirms the two phase coexistence at $r > 10$Å. However, it is clearly shown in Figure 10 that below 10 Å, *R3c* is the only phase group that correctly describes the local atomic distribution. Additionally, largest off-centering displacements of Na atoms and the most significant distortions in Na-O-Na correlations are indicated (similar to that shown in Figure 6), which is the result of the flexibility of Na atomic position. The radius of sodium ion is very small (1.02 Å)[24] whereas it is surrounded by 12 nearest oxygen atoms (1.40 Å in radius[24]) with the average Na-O distance of 2.79 Å. These oxygen atoms form a cage with very large space for an Na atom to move around. Of course, Nb atoms also have off-centered displacement, as believed conventionally. But the nominal ionic size of Nb (0.74 Å)[24] is much smaller for the volume of the octahedron formed by the six oxygens surrounding Nb. Thus the picture of Nb rattling in the O_6 cage is invalid.

Below 190K, $NaNbO_3$ falls in the ferroelectric state, with the parallel spontaneous polarization. Again, if we compare the PDF in the very short range (three red lines in Figure

7), namely within the size of the elemental perovskite unit cell, the splitting of the first peak confirms the Nb-O variations in the NbO_6 octahedra, one at r = 1.87Å and the other at r = 2.1Å, which is attributed to the off-centered displacement of Nb atom. Especially, the two Nb-O peaks are not identical and the ratio of their intensities is about 1.5. In some previous studies, Nb was considered to move towards the [111] direction of the NbO_6. But in such a case the split Nb-O peaks should have the 1:1 intensity ratio. Our PDF result seems to indicate that Nb moves towards a direction between (111) and (110). Moreover, with the evolution of temperature below 190K, the peaks of Nb-O bond lengths prefer to stay the same, but the Na-O bond correlation peak shifts very significantly. During cooling, the amplitude of thermal vibration of Na becomes very small, which leaves Na to more clearly off-centered positions. At 15K, two well-defined Na-O peaks are formed at r = 2.4 Å and r = 3.1 Å, inferring that Na atoms have about 14% off-centering from the center of the oxygen cage, much larger than the off-centering of Nb atoms. Also, the ratio of the intensities of these two peaks is again about 1.5, though the intensities are relatively small due to broadening of average Na-O correlations. That means Na may have a similar direction of movement as Nb. The coincidence of Na and Nb off-center displacements contribute to the formation of large dielectric polarization.

From 490K to 300K, the space group at short range is always *R3c*, which is a ferroelectric (FE) state. However, the structure over the long distance beyond 10 Å is always antiferroelectric (AFE) with the *Pbcm* group symmetry. This can only mean that nano-scale twins are formed in the *R3c* phase with the ferroelectric polarization changing from one twin

to another. Above room temperature, this kind of average AFE structure appears through the whole lattice. Below 190K, some of the FE domains are larger, while much of the FE domains remain in the nano-scale twins, resulting in apparent coexistence of the *R3c* and *Pbcm* phases.

The results of PDF fitting clearly indicate that the true ground state for the local structure of $NaNbO_3$ below 490K is actually the *R3c* structure. It is the real phase of $NaNbO_3$ at low temperatures, but they tend to form nano-twins, resulting in the appearance of the *Pbcm* phase at long ranges. It should be noted that if the twins are regularly spaced they should result in superlattice diffraction, and a different structure with a large unit cell. That such superlattice diffraction peaks are not observed implies the spacings of nano-twins are irregular. As noted by Hendrick and Teller[25] for partially ordered layered lattices of graphite, such irregular, random arrangement of twins can produce sharp diffraction peaks with the average lattice structure, in this case *Pbcm*, rather than broad diffraction patterns corresponding to the short structural coherence length.

The most probable cause of the formation of nano-twins is the low mobility of Na ions at low temperatures. The off-centering of Na is quite large, as much as 0.4 Å, greatly contributing to large ferroelectric polarization. But at the same time the energy barrier to move from one off-centered position to another must be significant, resulting in trapping of Na ion in one of these off-centered positions at low temperatures. This makes formation of large FE domains difficult, resulting in nano-twin states. The large barrier for motion also explains the hysteric

effect naturally without invoking the idea of quantum paraelectricity[26]. On the other hand, as we mentioned earlier, replacing Na with other elements such as K can improve its ferroelectric and piezoresponse performance. The ionic radius of K^+ is larger than that of Na^+ by 0.25 Å[24], reducing the off-centering to only 0.1 Å. The energy barrier for such a small off-centering is negligible, making K^+ much more mobile than Na^+, although the contribution of K^+ to ferroelectricity is smaller. Apparently the new lead-free ferroelectric materials[4] were synthesized by improving the mobility of alkali-ion at the expense of losing some polarization, by partially replacing Na by K.

Conclusions

In summary, we have discovered the local aspect of evolution of the structure and space group of sodium niobate from 930K down to 15K through the combination of the standard neutron scattering diffraction Rietveld analysis and the local pair distribution function (PDF) study. The long-range crystallographic phase undergoes seven phase transitions, through cubic, tetragonal, orthorhombic and rhombohedral. However, the study of the short-range structure demonstrates that in spite of such complexity there are only three main patterns in the local structures, as shown in Figure 7. At high temperatures (above 490K) local dielectric polarization is absent. In the intermediate temperature range (down to 300K) Nb starts to become off-centered, but Na remains centered. Only below 300K both Nb and Na become off-centered. The study of the local structure brought further new information. Especially at low temperatures, in which $NaNbO_3$ experiences antiferroelectric and ferroelectric transitions, our local PDF shows that the short-distance structure is always in the *R3c* space group, which

is actually the real groud state. In the long-range, however, the nano-twined structure of the *R3c* cells brings the appearance of the *Pbcm* space group. Our discovery solves the long-standing controversies in numerous neutron studies of sodium niobate at low temperature and explains why $NaNbO_3$ is a good base compound for promising new ferroelectric materials which can substitute lead-containing toxicant materials.

Acknowledgment

This work was supported by the National Science Foundation through DMR-0602876. The work at the Manuel Lujan Neutron Science Center at Los Alamos National Laboratory was supported by the U.S. Department of Energy, Office of Science, Office of Basic Energy Sciences.

Figure captions

Figure 1. Evolution of the neutron diffraction patterns for $NaNbO_3$ as temperature is varied from 930K to 15K. Each pattern is representative for one phase of $NaNbO_3$. Superlattice peaks are marked with arrows.

Figure 2. Observed (solid spheres), calculated (open circles), and difference (crosses) profiles obtained after the Rietveld refinement of $NaNbO_3$ using the mixture pf phases with rhombohedra *R3c* group (70%) and orthorhombic *Pbcm* group (30%) at 15K. Peaks marked with arrows are the ones belong only to the *R3c* group according to the analysis of GASA software.

Figure 3. Neutron pair distribution function $G(r)$ analysis of $NaNbO_3$ at 820K with the *Cmcm* parameters from the Rietveld analysis. This phase is well described by the *Cmcm* structure. Models obtained by the Rietveld analysis can fit the PDF from 930K to 600K quite well. This is an example which shows the accuracy of the Rietveld model at high temperatures.

Figure 4. Neutron pair distribution function $G(r)$ analysis of $NaNbO_3$ at 490K with the *Pbcm* group. Note that this structure model can describe the PDF only above 5.2Å.

Figure 5. Neutron pair distribution function $G(r)$ analysis of $NaNbO_3$ at 490K with the *R3c* group. Note that this phase can describe the structure profile only below 5.2Å

Figure 6. (a) Atomic arrangement of $NaNbO_3$ at 490K. Yellow balls are Na, green balls are niobium and purple balls are oxygen. *a* and *b* are *R3c* axes and *a*' and *b*' are *Pbcm* axes. (b) Construction of the basic cells (~ 4 Å) and local polarizations, and every arrow corresponds to a spontaneous polarization in an elementary perovskite cell.

Figure 7. Neutron pair distribution function $G(r)$ analysis of $NaNbO_3$ from 930K to 15K up to 4Å. Note that the result can be divided into three groups with the evolution of temperature: 900K-600K(green lines), 490K-300K(blue lines) and 190K-15K(red lines). This indicates only two basic structural changes happen at a short range. Peaks resulted from Na-O and Nb-O bonds are marked with arrows and obvious Nb-O bond lengths change at very short distance from 490K to 15 K are also emphasized.

Figure 8. Depictions of NaO_{12} at 930K (left top) and at 15K (left bottom), and NbO_6 at 930K (right top) and at 15K (right bottom) according to the PDF analysis. Na and Nb displacements are exaggerated for clarity.

Figure 9. Neutron PDF analysis of $NaNbO_3$ at 15K with *R3c* and *Pbcm* group coexistence model from the Rietveld analysis. Note that the differences gradually vanish above 10Å.

Figure 10. Neutron pair distribution function $G(r)$ analysis of $NaNbO_3$ at 15K with only the *R3c* group. Note that the differences are very small below 10Å and begin to become obvious above 10Å.

Table Captions:

Table 1. Phase evolution of $NaNbO_3$ at various temperatures.

Table 2. Structural parameters of $NaNbO_3$ obtained by the Rietveld analysis from 930 K to 15 K.

References

1. R. E. Jaeger, and L. Egerton, J. Am. Ceram. Soc. **45**, 209 (1962).
2. R. H. Dungan, and R. D. Golding, J. Am.Ceram. Soc. **48**, 601 (1965).
3. G. H. Haertling, J. Am. Ceram. Soc. **50**, 329–330 (1967).
4. Y. Saito, H. Takao, T. Tani, T. Nonoyama, K. Takatori, T. Homma, T. Nagaya and M. Nakamura, Nature **432,** 84 (2004).
5. C. N. W. Darlington and K. S. Knight, Physica B **266**, 368 (1999).
6. M. Ahtee, A M. Glazer, and H. D Megaw, Philos. Mag. **26**, 995 (1972).
7. I. Lefkowitzk, K. Lukazewicz, and H. D. Megaw, Acta. Crystllogr. **20**, 670 (1966).
8. O. Di´eguez, K. M. Rabe, and D.Vanderbilt, Phys. Rev. B **72**, 144101(2005).
9. Y. Shiratori, A. Magrez, W. Fischer, J. Phys. Chem. C **111**, 18493 (2007).
10. Helen D. Megaw, Ferroelectrics, **7**, 87 (1974)
11. C. N. W. Darlington and K. S. Knight, Physica B **266**, 368 (1999)
12. C. N. W. Darlington and H. D. Megaw, Physica B **29**, 2171 (1973)

13. C. N. W. Darlington, Solid State Commun. **29**, 307 (1979)
14. K. Lukazewicz, and H. D. Megaw, Acta Crystallogr. B **25**, 851 (1969)
15. I. Tomeno, Y. Tsunoda, K. Oka, M. Matsuura, and M. Nishi, Phys. Rev. B **80,** 104101 (2009)
16. W. Zhong and D. Vanderbilt, Phys. Rev. Lett. **74**, 2587 (1995)
17. O. Di´eguez, K. M. Rabe, and D. Vanderbilt, Phys. Rev. B **72**, 144101(2005)
18. S. K. Mishra, R. Mittal, Phys. Rev. B **83**, 134105 (2011)
19. S.K. Mishra, N. Choudhury, Phys. Rev. B **76**, 024110 (2007)
20. N.W. Thomas, Acta Crystallogr. Sect. B, Volume **52**, Part 1 (1996)
21. O. Hanske-Petitpierre, Y. Yacoby, J. M. De Leon, Phys. Rev. B **44**, 6700 (1991)
22. VA Shuvaeva, K Yanagi, K Yagi, K Sakaue, Solid State Commun. **106**, 335 (1998)
23. T. Egami and S. J. L. Billinge, "Underneath the Bragg peaks: Structural analysis of complex materials" (Pergamon, Oxford, 2003)
24. R. D. Shannon, Acta Crystallogr. Sect. A **32**, 751 (1976)
25. S. Hendricks and E. Teller, J. Chem. Phys. **10**, 147 (1942)
26. S. I. Raevskaya, I. P. Raevski, S. P. Kubrin, M. S. Panchelyuga, V. G. Smotrakov, V. V. Eremkin and S. A. Prosandeev, J. Phys: Cond. Matter **20,** 232202 (2008).

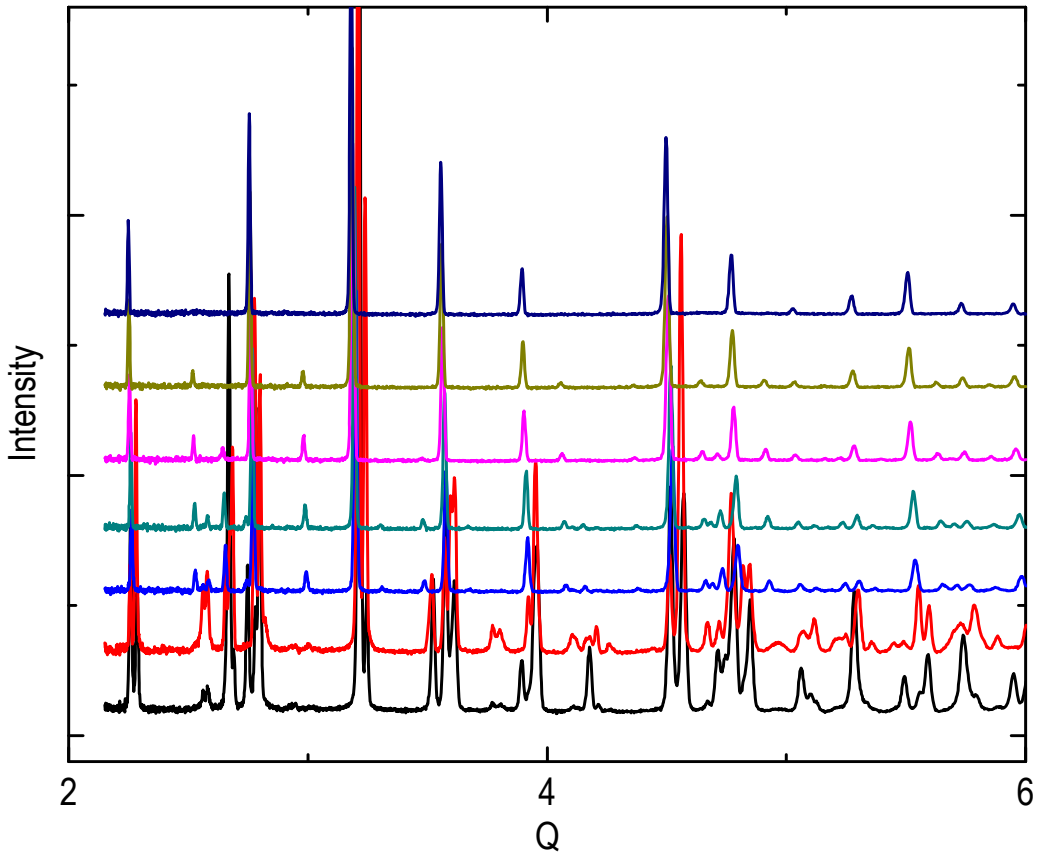

Fig. 1

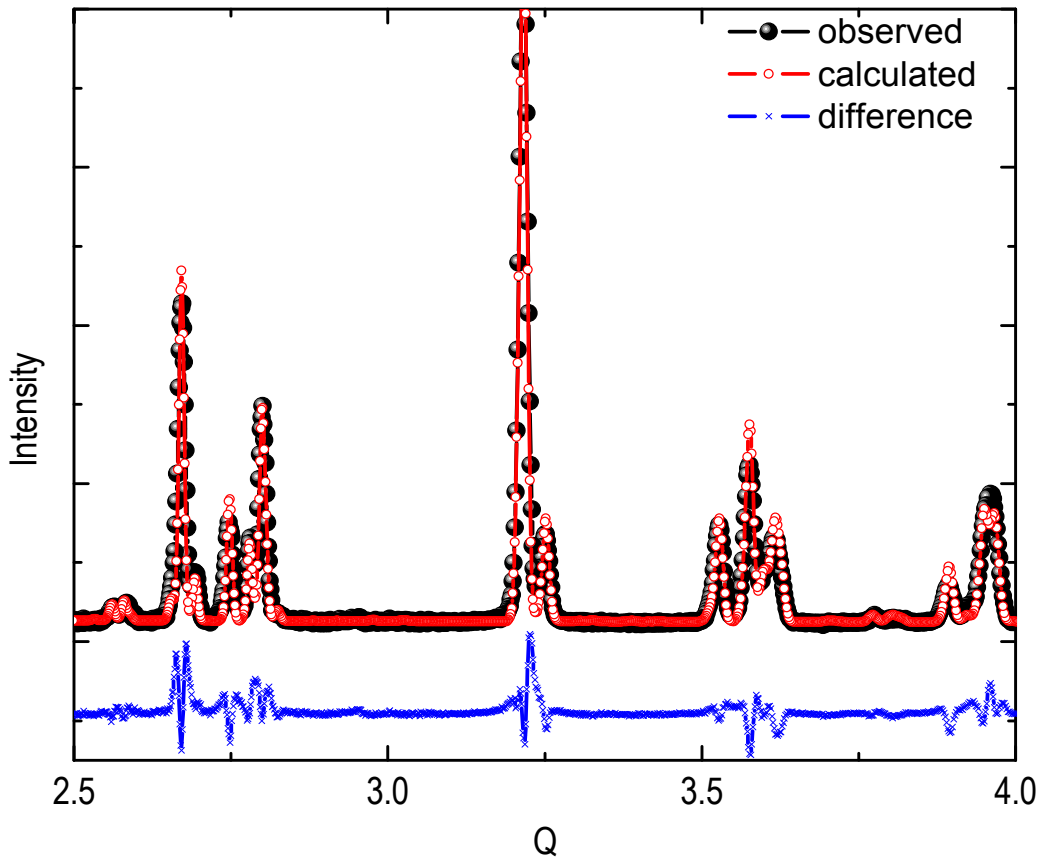

Fig. 2

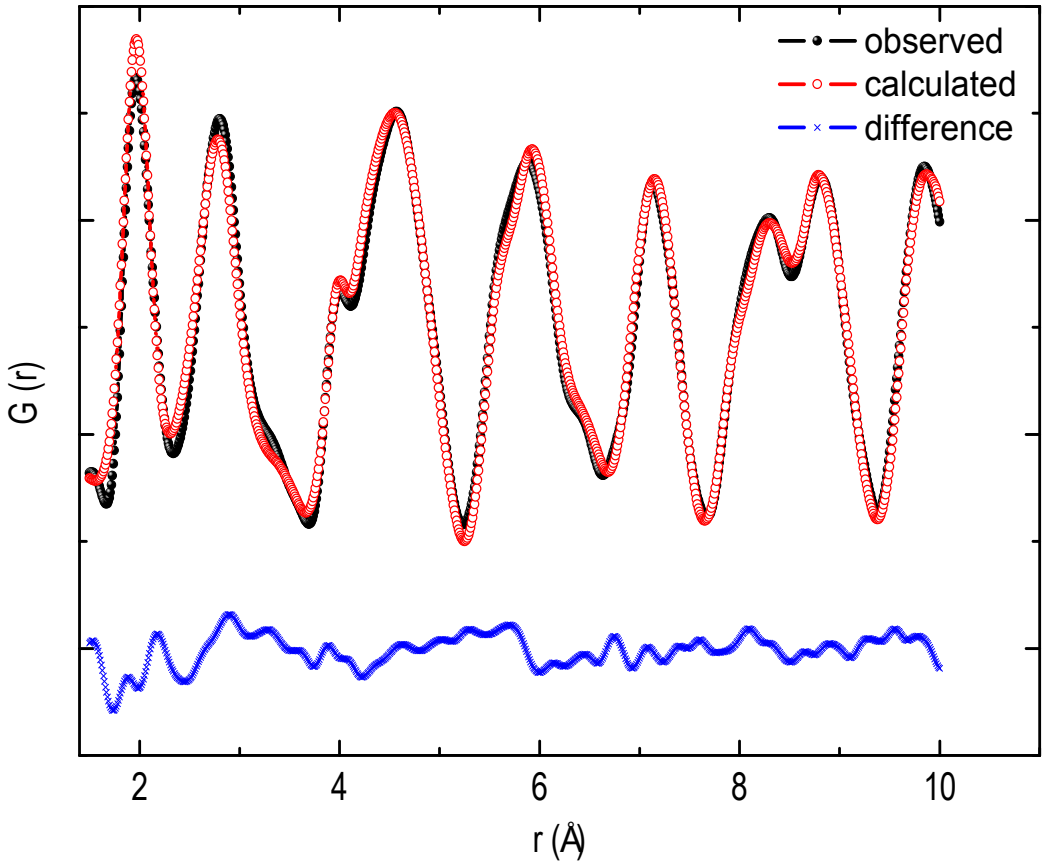

Fig. 3

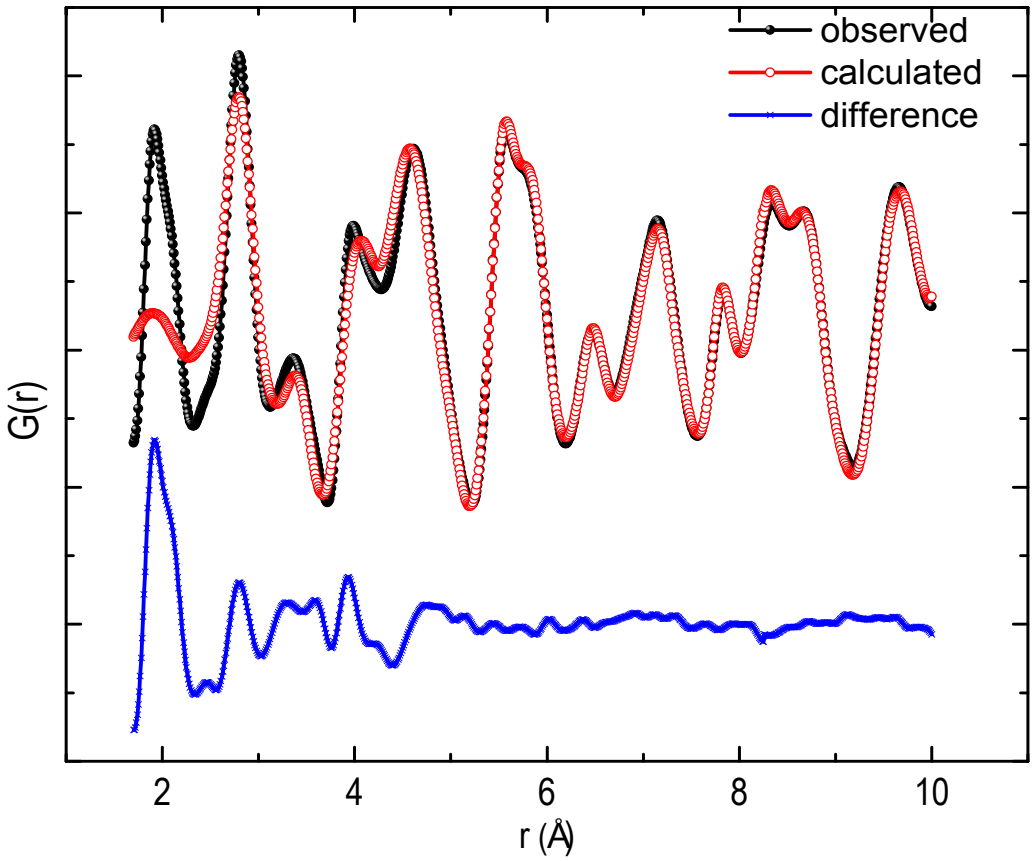

Fig. 4

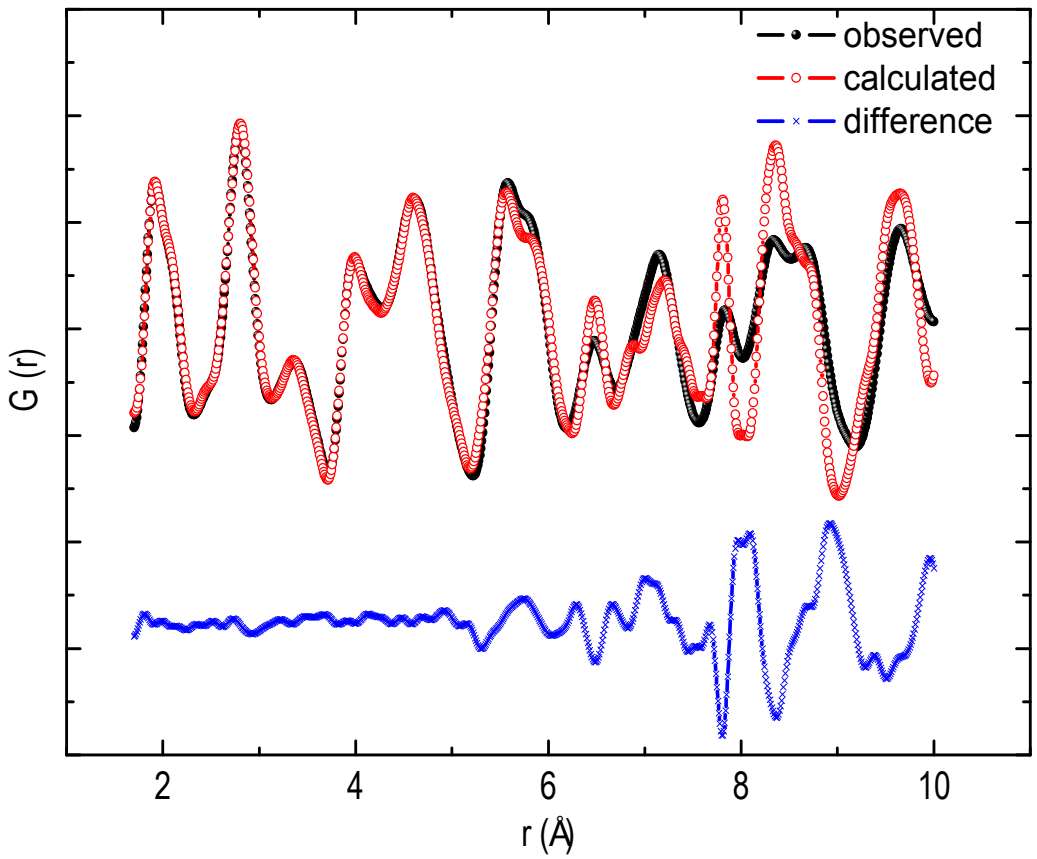

Fig. 5

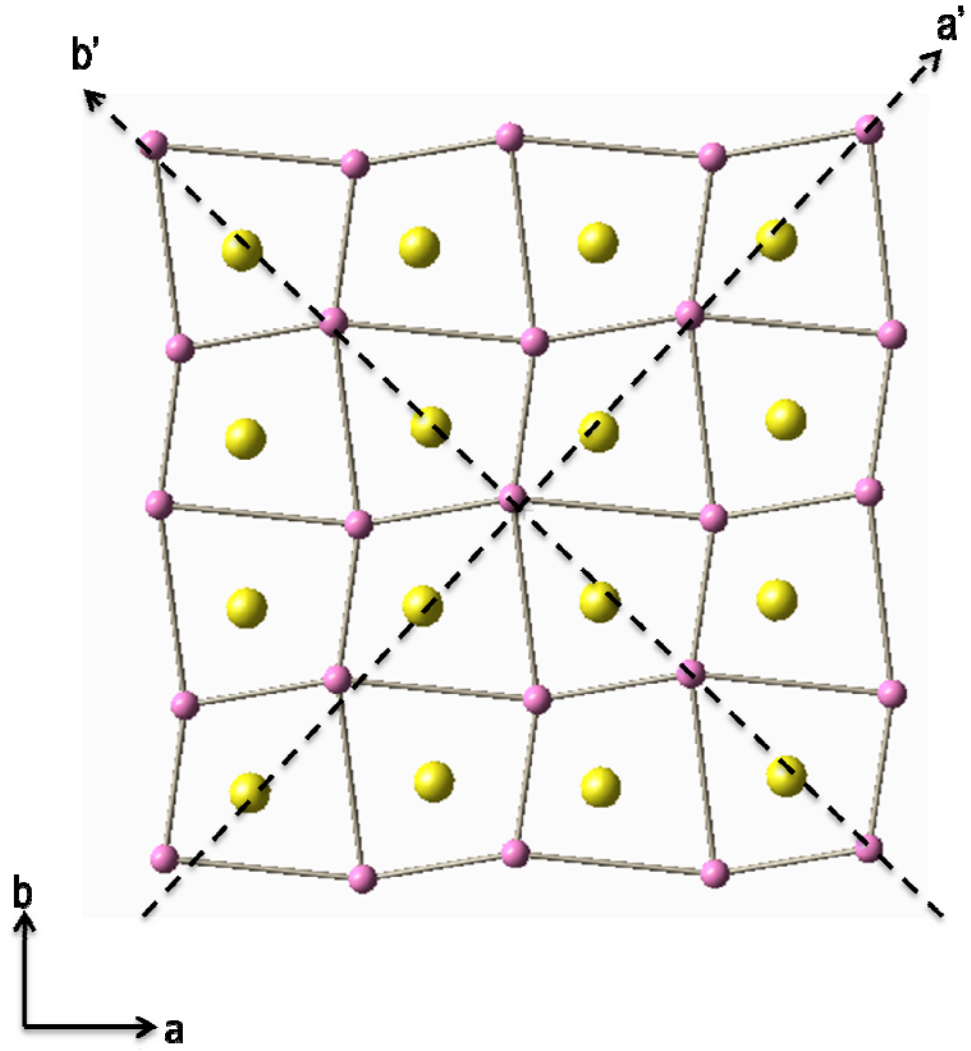

Fig. 6 (a)

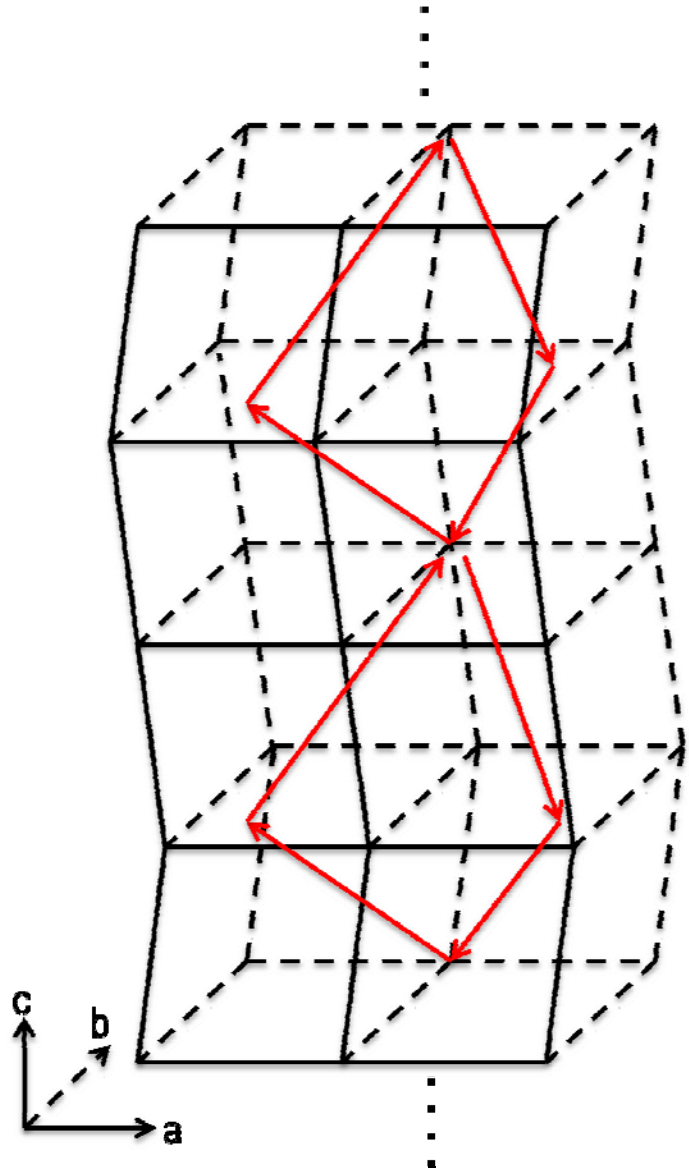

Fig. 6 (b)

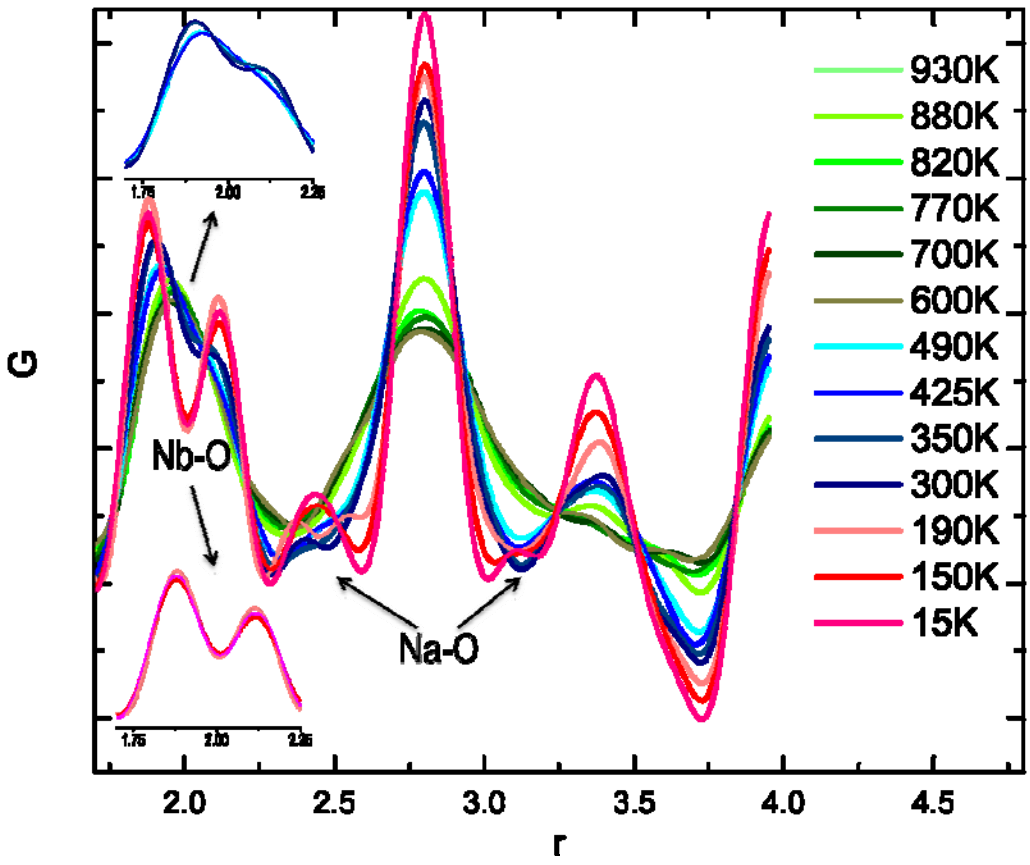
G
r
Nb-O
Na-O
930K
880K
820K
770K
700K
600K
490K
425K
350K
300K
190K
150K
15K
2.0
2.5
3.0
3.5
4.0
4.5

Fig. 7

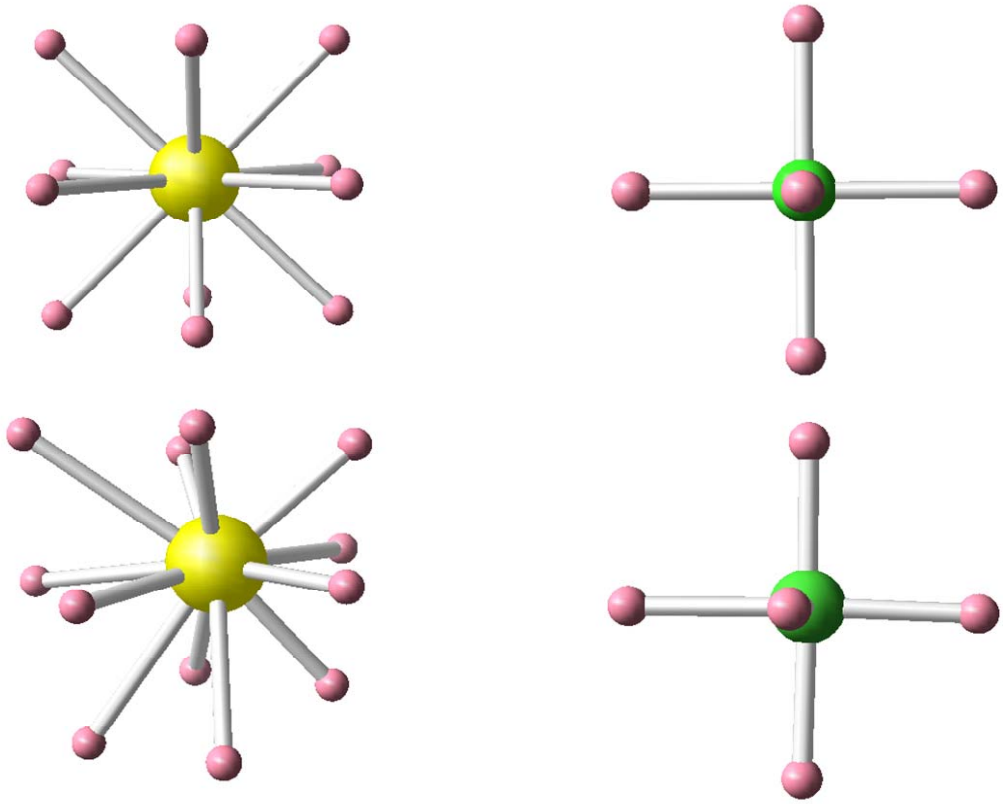

Fig. 8

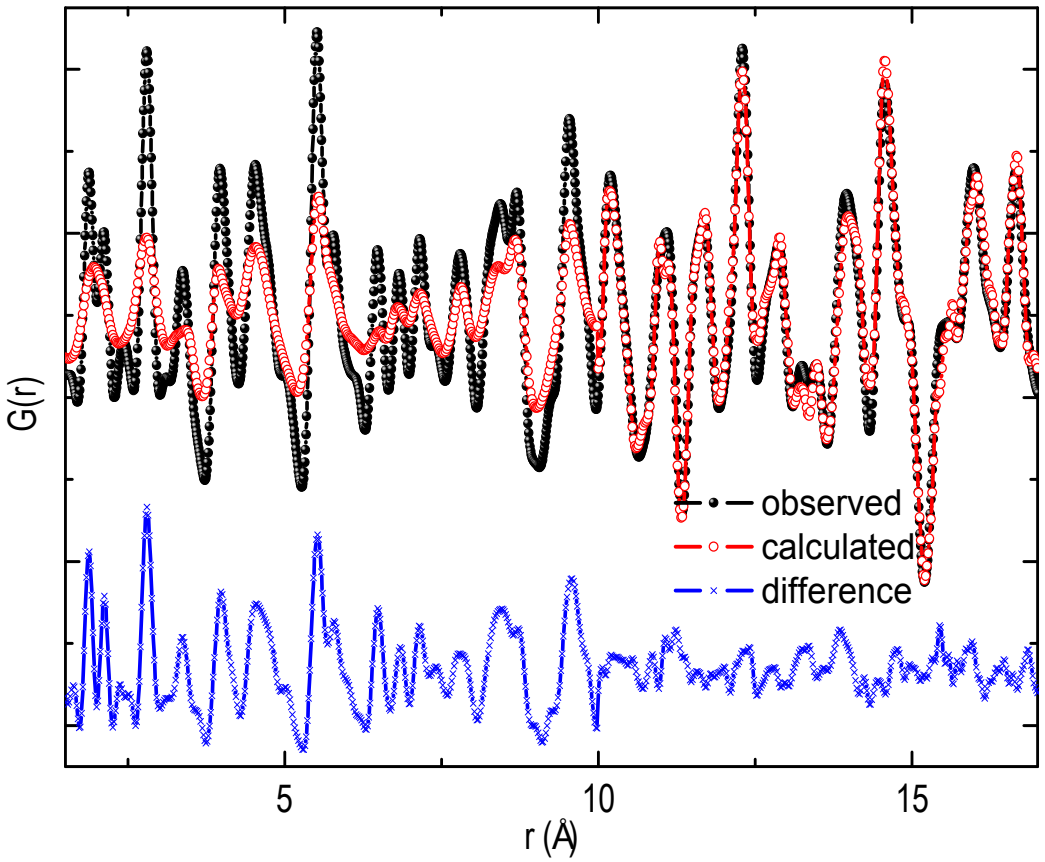

Fig. 9

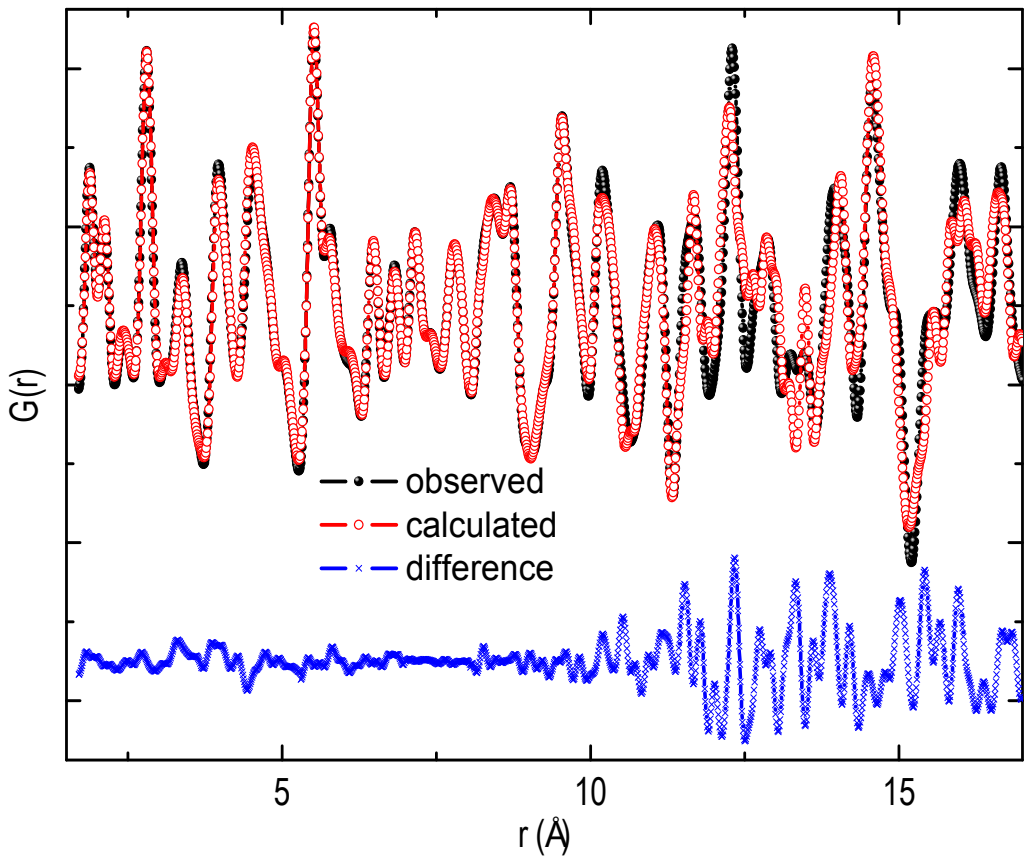

Fig. 10

Table 2

Temperature: 930K

Atoms	X	Y	Z	Uiso
Na	0	0	0	0.0531
Nb	0.5	0.5	0.5	0.01331
O	0	0.5	0.5	0.04169

Lattice parameters (Å)
a=*b*=*c*=3.9507 *α*=*β*=*γ*=90°

Agreement factor
wRp=0.0667 Rp=0.0469
CHI**2=8.495 RF**2=0.1596

Temperature: 880K

Atoms	X	Y	Z	Uiso
Na	0	0.5	0.5	0.06416
Nb	0	0	0	0.02759
O1	0	0	0.5	0.03643
O2	0.2754	0.2247	0	0.03643

Lattice parameters (Å)
a=*b*=5.5786, *c*=3.9510 *α*=*β*=*γ*=90°

Agreement factor
wRp=0.0667 Rp=0.0469
CHI**2=

Temperature: 700K

Phase 1(Cmcm)

Atoms	X	Y	Z	Uiso
Na1	-0.0074	0	0.25	0.04329
Na2	0.4926	0	0.25	0.04329
Nb	0.75	0.75	0	0.02401
O1	0	-0.2844	0	0.02216
O2	-0.2304	0	-0.0691	0.02216
O3	0.7546	-0.2574	0.25	0.02216

Lattice parameters (Å)
a=7.8705, *b*=7.8605, *c*=7.8681
α=*β*=*γ*=90°

Phase 2(Pbnm)

Atoms	X	Y	Z	Uiso
Na1	0.6867	0.8774	0.25	0.02367
Na2	1.1592	0.3899	0.1155	0.02367
Nb1	0.5	0	0	0.00499
Nb2	0.5242	-0.0321	0	0.00812
O1	-0.5049	-0.0079	0.25	0.08941
O2	0.0332	-0.5012	0.1338	0.08941
O3	0.7288	0.263	0.0543	0.08941
O4	0.6805	0.312	0.3894	0.08941
O5	0.6886	0.3073	0.7237	0.08941

Lattice parameters (Å)
a=5.3688, *b*=5.8333, *c*=23.56499
α=*β*=*γ*=90°

Agreement factor
wRp=0.1059, Rp=0.0644, CHI**2=20.35, RF**2=0.2990

Phase ratio
Phase1=4.5% Phase2=95.5%